

Advancing Supervised Learning with the Wave Loss Function: A Robust and Smooth Approach

Mushir Akhtar^a, M. Tanveer^{a,*}, Mohd. Arshad^a, for the Alzheimer's Disease Neuroimaging Initiative^{**}

^a*Department of Mathematics, Indian Institute of Technology Indore, Simrol, Indore, 453552, India*

Abstract

Loss function plays a vital role in supervised learning frameworks. The selection of the appropriate loss function holds the potential to have a substantial impact on the proficiency attained by the acquired model. The training of supervised learning algorithms inherently adheres to predetermined loss functions during the optimization process. In this paper, we present a novel contribution to the realm of supervised machine learning: an asymmetric loss function named wave loss. It exhibits robustness against outliers, insensitivity to noise, boundedness, and a crucial smoothness property. Theoretically, we establish that the proposed wave loss function manifests the essential characteristic of being classification-calibrated. Leveraging this breakthrough, we incorporate the proposed wave loss function into the least squares setting of support vector machines (SVM) and twin support vector machines (TSVM), resulting in two robust and smooth models termed as Wave-SVM and Wave-TSVM, respectively. To address the optimization problem inherent in Wave-SVM, we utilize the adaptive moment estimation (Adam) algorithm, which confers multiple benefits, including the incorporation of adaptive learning rates, efficient memory utilization, and faster convergence during training. It is noteworthy that this paper marks the first instance of Adam's application to solve an SVM model. Further, we devise an iterative algorithm to solve the optimization problems of Wave-TSVM. To empirically showcase the effectiveness of the proposed Wave-SVM and Wave-TSVM, we evaluate them on benchmark UCI and KEEL datasets (with and without feature noise) from diverse domains. Moreover, to exemplify the applicability of Wave-SVM in the biomedical domain, we evaluate it on the Alzheimer's Disease Neuroimaging Initiative (ADNI) dataset. The experimental outcomes unequivocally reveal the prowess of Wave-SVM and Wave-TSVM in achieving superior prediction accuracy against the baseline models. The source codes of the proposed models are publicly available at <https://github.com/mtanveer1/Wave-SVM>.

Keywords: Supervised learning, Pattern classification, Loss function, Support vector machine, Twin

*Corresponding author

**The data for this article were sourced from the Alzheimer's Disease Neuroimaging Initiative (ADNI) database (adni.loni.usc.edu). While investigators within the ADNI contributed to the design and implementation of ADNI and provided data, they were not involved in the analysis or writing of this report.

1. Introduction and Motivation

In the realm of machine learning, supervised learning stands as a cornerstone, which empowers to build models that can make accurate predictions and classifications. A critical component within this paradigm is the choice of an appropriate loss function, which plays a crucial role in guiding the training process. The loss function quantifies the disparity between predicted outcomes and true labels, providing an evident indication of a model's performance [1]. Its role extends beyond mere evaluation; it fundamentally shapes the model's learning trajectory, influencing its generalization ability, and aligning its predictions with the intrinsic goals of the task.

Support Vector Machine (SVM) [2] emblematic of a stalwart supervised learning algorithm. It is grounded in the principle of structural risk minimization (SRM) and originates from statistical learning theory (SLT), consequently having a solid theoretical foundation and demonstrating better generalization capabilities. It has extensive applications across various domains, such as image classification [3], wind speed prediction [4], face recognition [5], handwritten digit recognition [6], and so forth.

Consider the training set $\mathcal{D} = \{x_i, y_i\}_{i=1}^l$, where $x_i \in \mathbb{R}^n$ represents the sample vector and $y_i \in \{-1, 1\}$ signifies the corresponding class label associated with the sample. The core idea that serves as the foundation of SVM involves the construction of a decision hyperplane $w^\top x + b = 0$, where $b \in \mathbb{R}$ represents the bias and $w \in \mathbb{R}^n$ signifies the weight vector. These parameters are estimated through the process of training using available data. For a test data point \tilde{x} , the associated class label \tilde{y} is predicted as 1 if $w^\top \tilde{x} + b \geq 0$ and -1 otherwise. The pursuit of an optimal hyperplane hinges upon two distinct scenarios within the input space: first, when training data is linearly separable, and second, when training data is linearly inseparable.

For a linearly separable scenario, the process of attaining the optimal parameters w and b involves addressing the following SVM model:

$$\begin{aligned} \min_{w,b} \quad & \frac{1}{2} \|w\|^2 \\ \text{subject to} \quad & y_i (w^\top x_i + b) \geq 1, \quad \forall i = 1, 2, \dots, l. \end{aligned} \tag{1}$$

The model described in equation (1) is named as hard-margin SVM, as it mandates the correct classification of each individual training sample. In cases where the data is linearly inseparable, the commonly employed strategy involves allowing for misclassification while imposing penalties for these errors. This is achieved by incorporating a loss function into the objective function, which leads to the subsequent unconstrained

optimization problem:

$$\min_{w,b} \frac{1}{2} \|w\|^2 + C \sum_{i=1}^l \mathfrak{L}(1 - y_i (w^\top x_i + b)), \quad (2)$$

where $C > 0$ is a trade-off parameter and $\mathfrak{L}(u)$ with $u := 1 - y_i (w^\top x_i + b)$ denotes the loss function. Since model (2) permits the misclassification of samples, it is identified as a soft-margin SVM model [2]. The objective of SVM is to obtain an optimal hyperplane that separates data points of distinct classes by maximum possible margin. This primarily involves solving a quadratic programming problem (QPP) whose complexity is proportional to the cube of the training dataset size. Twin SVM (TSVM) [7], a variant of the SVM, tackles this problem by solving two smaller QPPs instead of one large QPP, thereby reducing computational costs by approximately 75% compared to traditional SVM methods. To enhance the generalization performance of TSVM, several variants have been proposed in the literature. As an example, to tackle the imbalance problem, Ganaie et al. [8] proposed the large-scale fuzzy least squares TSVM. Further, to address the noise-sensitivity of TSVM Tanveer et al. [9] proposed the large-scale pin-TSVM by utilizing the pinball loss function. Both of the aforementioned algorithms eliminate the requirement of matrix inversion, making them suitable for large-scale problems. To delve deeper into the variants of TSVM models, readers can refer to [10].

Extensive research endeavors have been dedicated to the development of novel loss functions for the purpose of enhancing the effectiveness of SVM models. Based on the smoothness of loss functions, we classify them into two distinct classes. The first category encompasses loss functions characterized by their smoothness, while the latter consists of those with non-smooth attributes. Here, we only review a subset of widely recognized loss functions, chosen to provide sufficient motivation for the work presented in this paper.

1.1. Non-smooth loss functions

- **Hinge loss function:** SVM with hinge loss function (C-SVM) was first proposed by Cortes and Vapnik [2]. The mathematical expression for the hinge loss function is given as:

$$\mathfrak{L}_{hinge}(u) = \begin{cases} u, & u > 0, \\ 0, & u \leq 0. \end{cases} \quad (3)$$

Figure 1a depicts the visual representation of the hinge loss function. It is non-smooth at $u = 0$ and unbounded.

- **Pinball loss function:** To improve the efficacy of C-SVM, Huang et al. [11] proposed SVM with pinball loss function (Pin-SVM). The mathematical formulation of the pinball loss is expressed as:

$$\mathcal{L}_{pin}(u) = \begin{cases} u, & u > 0, \\ -\tau u, & u \leq 0, \end{cases} \quad (4)$$

where $\tau \in [0, 1]$. It penalizes both correctly classified and misclassified samples so that if there is noise near the decision boundary, it can be adjusted to strike a trade-off between accuracy and noise insensitivity. For $\tau = 0$, the pinball loss function (See Figure 1b) is reduced to the hinge loss function. It is also non-smooth at $u = 0$ and unbounded.

- **Ramp loss function:** To enhance the robustness of C-SVM against outliers, Brooks [12] incorporate the ramp loss function into the SVM setting. The mathematical representation of the ramp loss function is articulated as follows:

$$\mathcal{L}_{ramp}(u) = \begin{cases} \theta, & u \geq \theta, \\ u, & u \in (0, \theta), \\ 0, & u \leq 0, \end{cases} \quad (5)$$

where $\theta \geq 1$. It imposes a limitation on penalties beyond a specific threshold. The ramp loss function (see Figure 1c) is also non-smooth at $u = 0$ but bounded.

Some other non-smooth loss functions that have been incorporated into the framework of SVM to improve its efficiency include the rescaled hinge loss [13], generalized ramp loss [14], flexible pinball loss [15], and so forth.

1.2. Smooth loss functions

- **Squared hinge loss function:** To improve the smoothness of the hinge loss function, Cortes and Vapnik [2] also designed the smooth version of the hinge loss function termed as squared hinge loss. The mathematical expression of the squared hinge loss function is expressed as:

$$\mathcal{L}_{s-hinge}(u) = \begin{cases} u^2, & u > 0, \\ 0, & u \leq 0. \end{cases} \quad (6)$$

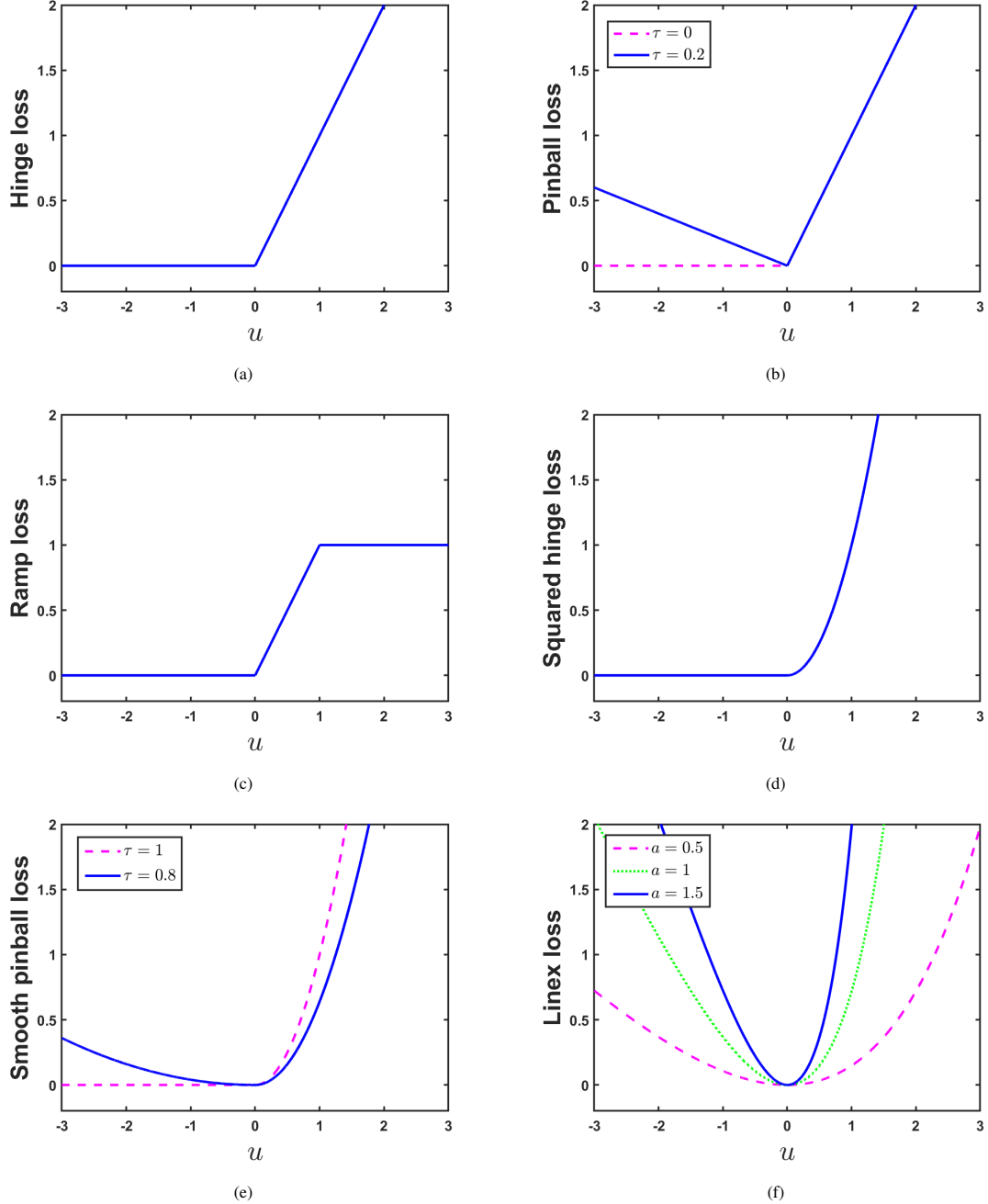


Figure 1: Visual illustration of baseline loss functions. (a) Hinge loss function. (b) Pinball loss function with $\tau = 0$ and $\tau = 0.2$. (c) Ramp loss function with $\theta = 1$. (d) Squared hinge loss function (e) Smooth pinball loss function with $\tau = 0.8$ and $\tau = 1$. (f) LINEX loss function with $a = 0.5$, $a = 1$, and $a = 1.5$.

Figure 1d presents the visual illustration of the squared hinge loss function. It is smooth and unbounded.

- **Smooth pinball loss function:** To enhance the insensitivity to noise of squared hinge loss function, Liu et al. [16] designed the smooth pinball loss function. The mathematical formulation of the smooth pinball loss is given as:

$$\mathfrak{L}_{s-pin}(u) = \begin{cases} (\tau u)^2, & u > 0, \\ [(1 - \tau)u]^2, & u \leq 0, \end{cases} \quad (7)$$

where $\tau \in [0, 1]$. For $\tau = 1$, the smooth pinball loss function (see Figure 1e) is reduced to the squared hinge loss function. It is also smooth and unbounded.

- **LINEX loss function:** LINEX loss is an asymmetric function that combines linear and exponential components [17]. Due to the merits of LINEX loss, Ma et al. [18] first incorporated it into the SVM framework and introduced a fast SVM model named LINEX-SVM. The mathematical expression for the LINEX loss is given as:

$$\mathfrak{L}_{LINEX}(u) = e^{au} - au - 1, \quad \forall u \in \mathbb{R}, \quad (8)$$

where $a \neq 0$ is the loss parameter that controls the penalty for classified and misclassified samples. Figure 1f presents the visual illustration of the LINEX loss function. It is smooth and unbounded.

- **RoBoSS loss function:** To enhance the robustness against outliers of smooth and unbounded loss functions, Akhtar et al. [19] proposed the RoBoSS loss function. The mathematical formulation of RoBoSS loss is given as follows:

$$\mathfrak{L}_{rbss}(u) = \begin{cases} \lambda(1 - (au + 1)e^{-au}), & u > 0, \\ 0, & u \leq 0, \end{cases} \quad (9)$$

where $a > 0, \lambda > 0$ are shape and bounding parameters, respectively. It is smooth and bounded.

In addition to these, recent advancements in smooth loss functions include the smooth truncated H ϵ loss [20], HawkEye loss [21], and so forth.

Through a comparative analysis of prevalent loss functions in the existing literature, we find that bounded loss functions demonstrate robustness by imposing a fixed penalty on all misclassified instances

beyond a specified margin. Further, the strategic imposition of penalties upon both correctly classified and misclassified samples facilitates the calibration of a delicate equilibrium between accuracy and resistance against noise. In addition to robustness to outliers and insensitivity towards noise, smoothness is also a crucial aspect of loss function. Generally, SVM utilizes non-smooth loss functions, which suffer from high computational costs as they have to solve a QPP. It is evident that if the loss function is not smooth, SVM is also not smooth [22]. Most of the robust and insensitive to noise models are not convex, so the optimization problem of these models cannot be solved using the Wolfe dual method. The convenience of the smooth loss function is that there are fast optimization techniques that are specific to smooth models.

Taking inspiration from prior research endeavors, this article proposes a novel asymmetric loss function, referred to as the wave loss function (see Figure 2). It is precisely engineered to exhibit robustness against outliers, insensitivity to noise, and a propensity for smoothness. Subsequently, by integrating the proposed wave loss into the least squares framework of SVM and TSVM, we present two novel models, namely Wave-SVM and Wave-TSVM. The optimization problem associated with the Wave-SVM is effectively addressed through the utilization of the adaptive moment estimation (Adam) algorithm. Further, to solve the optimization problems of the Wave-TSVM an efficient iterative algorithm is utilized. The major contributions of this paper can be outlined as follows:

- We propose a novel asymmetric loss function named wave loss, designed to exhibit robustness against outliers, insensitivity to noise, and smooth characteristics. Further, we delve into the theoretical aspect of the wave loss function and validate its capability to maintain a vital classification-calibrated property.
- We amalgamate the proposed wave loss function into the least squares setting of SVM and TSVM and introduce two novel robust and smooth models, termed Wave-SVM and Wave-TSVM, respectively.
- We address the optimization problem inherent to Wave-SVM by employing the Adam algorithm, known for its lower memory requirements and efficacy in handling large-scale problems. To our knowledge, this is the first time Adam has been used to solve an SVM problem. Further, we utilized an efficient iterative algorithm to solve the optimization problems of Wave-TSVM.
- We perform comprehensive numerical experiments using benchmark UCI and KEEL datasets (with and without feature noise) from various domains. The outcomes vividly showcase the outstanding performance of the proposed Wave-SVM and Wave-TSVM when contrasted with baseline models.
- To demonstrate the superiority of the proposed Wave-SVM and Wave-TSVM models in the biomed-

cal realm, we conducted experiments using the ADNI dataset. These empirical investigations furnish substantial evidence of the proposed models applicability in real-world medical scenarios.

The rest of this paper is structured as follows: Section 2 presents the proposed wave loss function and elucidates its distinctive characteristics. Further, Section 2 provides the formulations of Wave-SVM and Wave-TSVM, along with an analysis of their computational complexity. Section 3 showcases the numerical findings. Lastly, Section 4 offers conclusions and outlines future research directions.

2. Proposed work

In this section, we introduce a groundbreaking asymmetric loss function named wave loss and elucidate its distinctive characteristics. Subsequently, we amalgamate the proposed wave loss into the frameworks of SVM and TSVM within the least squares setting and propose two novel models, namely Wave-SVM and Wave-TSVM. We also analyze the computational complexity associated with the proposed algorithms.

2.1. Wave loss function

We present a substantial advancement within the domain of supervised learning: a novel asymmetric loss function that embodies robustness against outliers, insensitivity to noise, and smoothness characteristics. This novel loss function, referred to as the wave loss function, is visually depicted in Figure 2. The mathematical expression of the proposed wave loss function is articulated as follows:

$$\mathfrak{L}_{\text{wave}}(u) = \frac{1}{\lambda} \left(1 - \frac{1}{1 + \lambda u^2 e^{au}} \right), \quad \forall u \in \mathbb{R}, \quad (10)$$

where $a \in \mathbb{R}$ is shape parameter and $\lambda \in \mathbb{R}^+$ is bounding parameter. The wave loss function (10), as delineated in this work, showcases the following inherent properties:

- It is robust to outliers and insensitive to noise. As it bound the loss to $1/\lambda$, which gives robustness to outliers, and it also gives loss to samples with $u \leq 0$, which produces insensitivity towards noise.
- It is non-convex, smooth, and bounded.
- It is infinitely differentiable and hence continuous for all $u \in \mathbb{R}$.
- For given value of λ , when $a \rightarrow +\infty$, the wave loss (10) converges point-wise to the “0 – 1/ λ ” loss which is defined as

$$\mathfrak{L}_{0-1}(u) = \begin{cases} \frac{1}{\lambda}, & u > 0, \\ 0, & u \leq 0. \end{cases}$$

Furthermore, when $\lambda = 1$ it converges to “0 – 1” loss.

- It has two advantageous parameters: shape parameter (a) determines the loss function’s shape, and bounding parameter (λ) sets thresholds for loss values.

It is crucial to note that the existing bounded loss functions set a strict limit on the maximum allowable loss for data points with substantial deviations. This effectively prevents noise and outliers from exerting excessive influence, thus enhancing the model’s robustness. However, the majority of the existing loss functions use a hard truncation strategy to bound the loss, which makes them non-smooth. In contrast, the proposed wave loss function is smooth and bounded simultaneously (refer to Figure 2). By adjusting the bounding parameter λ , the wave loss function smoothly bounds the loss to a predefined value. The primary benefit of the smoothness characteristic lies in its facilitation of the application of gradient-based optimization algorithms. This property ensures the existence of well-defined gradients, enabling the utilization of rapid and reliable optimization techniques.

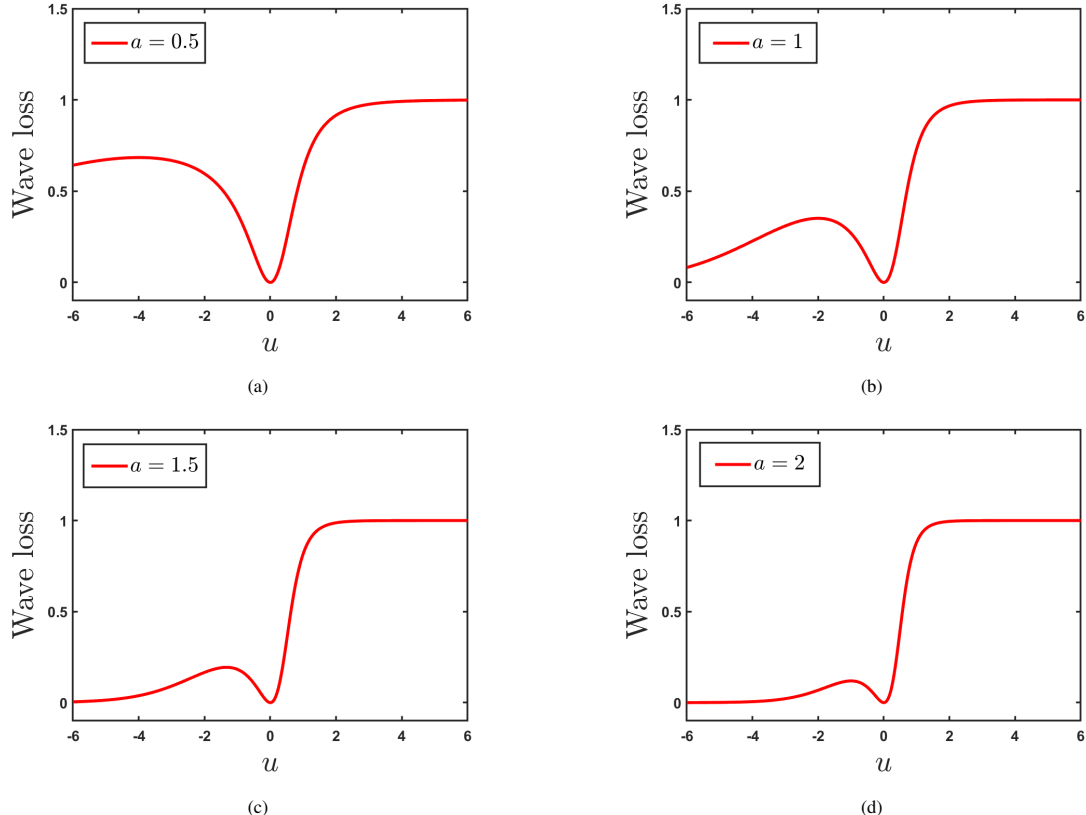


Figure 2: Illustration of wave loss function for fixed $\lambda = 1$ and different values of a . Subfigures (a), (b), (c), and (d) demonstrate that the value of a controls the strength of the penalty for correctly classified and misclassified samples.

2.2. Theoretical analysis of the wave loss function

In this subsection, we analyze the theoretical characteristics inherent to the proposed wave loss function and provide evidence to demonstrate that the wave loss function exhibits a crucial classification-calibrated property. Bartlett et al. [23] introduced the concept of classification-calibration to assess the statistical effectiveness of loss functions in the context of classification learning. It ensures that the model's predicted probabilities reflect the true likelihood of an event. For more details, readers can refer to [23, 24]. This attribute holds crucial importance in enhancing our understanding of the performance dynamics of the wave loss function within classification tasks.

Consider that the training data $\mathcal{D} = \{x_i, y_i\}_{i=1}^l$ is independently sampled from a probability distribution \mathbf{P} . The distribution \mathbf{P} is defined over a combined space of inputs and corresponding labels, where the input space X is a subset of \mathbb{R}^n and the label space Y consists of two possible labels: -1 and 1 . In this context, the main objective is to develop a binary classifier \mathbf{C} , which takes inputs from the space X and assigns them to one of the two labels in Y . The central goal of this classification problem is to design a classifier in a way that minimizes the associated error. The risk associated with a specific classifier \mathbf{C} is quantified by the following mathematical expression:

$$R(\mathbf{C}) = \int_X P(y \neq \mathbf{C}(x)|x) dP_X.$$

Here $P(y|x)$ signifies the probability distribution of the label y given an input x , and dP_X represents the marginal distribution of the input x according to the distribution \mathbf{P} . Moreover, the conditional distribution $P(y|x)$ is a binary distribution, implying it is determined by the probabilities $\text{Prob}(y = 1|x)$ and $\text{Prob}(y = -1|x)$. To ease in writing, we further utilize $P(x)$ and $1 - P(x)$ to represent $\text{Prob}(y = 1|x)$ and $\text{Prob}(y = -1|x)$, respectively. In simpler terms, the objective is to construct a classifier that accurately assigns labels to inputs while minimizing the overall error.

Now, the Bayes classifier, for $P(x) \neq 1/2$, is defined as follows:

$$f_{\mathbf{C}}(x) = \begin{cases} -1, & P(x) < 1/2, \\ 1, & P(x) > 1/2. \end{cases} \quad (11)$$

It can be verified that the Bayes classifier effectively minimizes the classification error. The following expression mathematically expresses the previous statement:

$$f_{\mathbf{C}} = \arg \min_{\mathbf{C}: X \rightarrow Y} R(\mathbf{C}).$$

Now, for any given loss function \mathfrak{L} , the expected error associated with a classifier $f: X \rightarrow \mathbb{R}$ is formulated as follows:

$$R_{\mathfrak{L}, P}(f) = \int_{X \times Y} \mathfrak{L}(1 - yf(x)) dP. \quad (12)$$

The function $f_{\mathfrak{L}, P}$, which minimizes the expected error over all measurable functions, is formulated as:

$$f_{\mathfrak{L}, P}(x) = \arg \min_{f(x) \in \mathbb{R}} \int_Y \mathfrak{L}(1 - yf(x)) dP(y|x), \quad \forall x \in X. \quad (13)$$

Subsequently, for the proposed wave loss $\mathfrak{L}_{wave}(\cdot)$, we can derive Theorem 2.1, providing evidence of the classification-calibrated nature [23] of the wave loss function. This characteristic, a valuable aspect of a loss function, ensures that the minimizer of expected error aligns with the sign of the Bayes classifier.

Theorem 2.1. *The proposed loss function $\mathfrak{L}_{wave}(u)$ is classification-calibrated, i.e., $f_{\mathfrak{L}_{wave}, P}$ has the same sign as the Bayes classifier.*

Proof. After simple computation, we arrive at the following outcome:

$$\begin{aligned} & \int_Y \mathfrak{L}_{wave}(1 - yf(x)) dP(y|x) \\ &= \mathfrak{L}_{wave}(1 - f(x))P(x) + \mathfrak{L}_{wave}(1 + f(x))(1 - P(x)) \\ &= \frac{1}{\lambda} \left(1 - \frac{1}{1 + \lambda(1 - f(x))^2 e^{a(1 - f(x))}} \right) P(x) + \frac{1}{\lambda} \left(1 - \frac{1}{1 + \lambda(1 + f(x))^2 e^{a(1 + f(x))}} \right) (1 - P(x)). \end{aligned}$$

In Figures 3a and 3b, the graphical representations of $\int_Y \mathfrak{L}_{wave}(1 - yf(x)) dP(y|x)$ are depicted as functions of $f(x)$, considering the cases when $P(x)$ is greater than 1/2 and when it is less than 1/2, respectively. As discernible from Figure 3, when $P(x)$ exceeds 1/2, the minimum value of $\int_Y \mathfrak{L}_{wave}(1 - yf(x)) dP(y|x)$ is achieved for a positive value of $f(x)$. Conversely, when $P(x)$ is less than 1/2, the minimum value corresponds to a negative value of $f(x)$.

Hence, it becomes evident from the patterns observed in Figures 3a and 3b that the proposed loss function $\mathfrak{L}_{wave}(u)$ holds the characteristic of being classification-calibrated. \square

2.3. Formulation of Wave-SVM

Through the amalgamation of the proposed wave loss function into the least squares setting of SVM, we construct a novel support vector classifier for large-scale problems that manifest robustness against outliers, insensitivity to noise, and smoothness characteristics. This advanced classifier is denoted as the

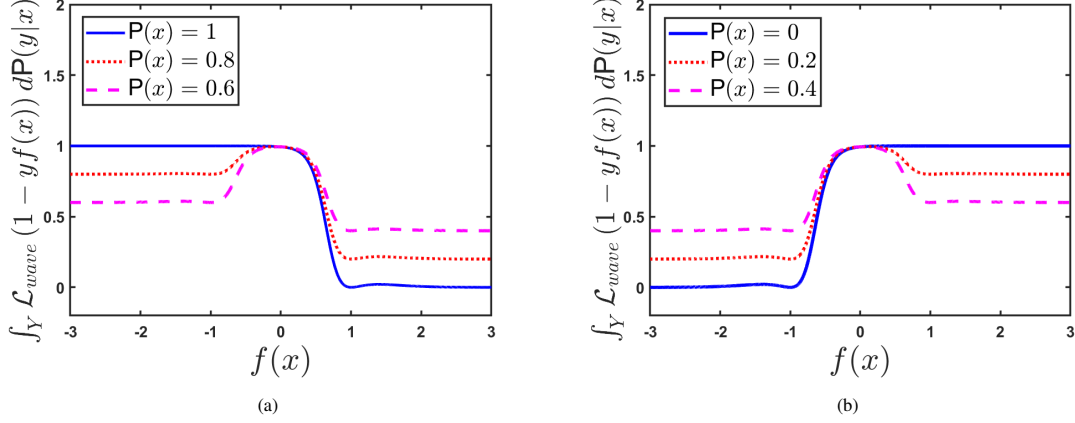


Figure 3: Illustrate the plot of $\int_Y \mathcal{L}_{wave} (1 - yf(x)) dP(y|x)$ over $f(x)$ with varying values of $P(x)$. (a) Depict the case where $P(x)$ is greater than $1/2$, and (b) illustrate the scenario where $P(x)$ less than $1/2$.

Table 1: Comparative Analysis of SVM Models Utilizing Different Loss Functions.

Models ↓ \ Characteristics →	Robust to outliers	Insensitive to noise	Sparse	Convex	Bounded	Smooth	Fast
C-SVM [2]	✗	✗	✓	✓	✗	✗	✗
Pin-SVM [11]	✗	✓	✗	✓	✗	✗	✗
LINEX-SVM [18]	✗	✓	✗	✓	✗	✓	✓
QTLS [25]	✗	✓	✗	✗	✗	✓	✓
FP-SVM [15]	✗	✓	✗	✓	✗	✗	✗
Wave-SVM (Proposed)	✓	✓	✗	✗	✓	✓	✓

Wave-SVM. For simplification, throughout the Wave-SVM formulation, we use the terminology w for $[w^\top, b]$ and x_i for $[x_i, 1]^\top$. The formulation of non-linear Wave-SVM is given as:

$$\min_{w, \xi} \quad \frac{1}{2} \|w\|^2 + C \sum_{i=1}^l \frac{1}{\lambda} \left(1 - \frac{1}{1 + \lambda \xi_i^2 e^{a \xi_i}} \right),$$

subject to $y_i (w^\top \phi(x_i)) = 1 - \xi_i, \forall i = 1, 2, \dots, l,$ (14)

where $C > 0$ is the regularization parameter, which determines the trade-off between margin and the penalty, λ and a are the parameters of the wave loss function, and $\phi(\cdot)$ is feature mapping associated with the kernel function. The characteristics of various SVM models, along with the Wave-SVM, are presented in Table 1, which showcases that the proposed Wave-SVM possesses most of the desirable attributes required for a better classifier.

The dual problem of the Wave-SVM is challenging to optimize due to the non-convexity of the wave loss function. However, the inherent smoothness of the Wave-SVM permits us to utilize a gradient-based algorithm to optimize the model. Gradient-based optimization with Wave-SVM offers several advantages. It facilitates faster convergence during training, as gradient-based methods generally converge at a faster rate than quadratic programming solvers [26]. In this paper, we adopt the Adam [27] optimization technique

for solving the Wave-SVM. It is an improved version of stochastic gradient descent with adaptive learning rates. This is the first time the Adam algorithm has been used to solve an SVM model. The Adam algorithm converges more quickly and stays stable during learning due to the adjustable learning rates. It combines the benefits of two other popular optimization algorithms: AdaGrad [28] and RMSProp [29]. The core idea behind Adam involves the computation of a progressively diminishing average for previous gradients and the squared gradients of the weights. Subsequently, based on these estimations, the algorithm establishes an adaptive learning rate for each weight parameter. It is important to note that the Adam algorithm only requires the gradient of the unconstrained optimization problem, and thus no modification was made to the Adam algorithm for its application to Wave-SVM.

2.3.1. Adam for linear Wave-SVM

For linear Wave-SVM, put $\phi(x) = x$ in equation (14), the linear Wave-SVM is defined as:

$$\min_w f(w) = \frac{1}{2} \|w\|^2 + C \sum_{i=1}^l \frac{1}{\lambda} \left(1 - \frac{1}{1 + \lambda \xi_i^2 e^{a \xi_i}} \right),$$

subject to $y_i (w^\top x_i) = 1 - \xi_i, \forall i = 1, 2, \dots, l.$ (15)

At each iteration t , k samples are chosen, and at that time the value of gradient, exponentially decaying averages of past gradients (first moment), and past squared gradients (second moment) are calculated using (16), (17), and (18), respectively as follows:

$$g_t = \nabla f(w) = w - \sum_{i=1}^k \frac{C y_i x_i \xi_i (2 + \xi_i) \exp(a \xi_i)}{\left[1 + \lambda \xi_i^2 \exp(a \xi_i) \right]^2}, \quad (16)$$

$$m_t = \beta_1 m_{t-1} + (1 - \beta_1) \nabla f(w_t), \quad (17)$$

$$v_t = \beta_2 v_{t-1} + (1 - \beta_2) \nabla f(w_t)^2, \quad (18)$$

where β_1 and β_2 are exponential decay rates for the first and second moment estimates, usually set to 0.9 and 0.999, respectively. Then, we compute the bias-corrected first and second moment estimates using (19) and (20), respectively.

$$\hat{m}_t = \frac{m_t}{(1 - \beta_1^t)}, \quad (19)$$

$$\hat{v}_t = \frac{v_t}{(1 - \beta_2^t)}. \quad (20)$$

In the end, the parameter w is updated as:

$$w_t = w_{t-1} - \alpha \frac{\hat{m}_t}{\sqrt{\hat{v}_t} + \epsilon}, \quad (21)$$

where α is the learning rate, and ϵ is a small constant used to avoid division by zero. Once the optimal w is achieved, the prediction regarding the label of the unknown sample x can be made using the decision function as:

$$\hat{y} = \text{sign}(f(x)) = \text{sign}(w^\top x). \quad (22)$$

2.3.2. Adam for non-linear Wave-SVM

The determination of the dual problem in the proposed Wave-SVM poses challenges that limit the applicability of kernel methods. In this case, to enhance the capacity of Wave-SVM for non-linear adaptation, we use the representer theorem [30], which allows us to express w in equation (14) as follows:

$$w = \sum_{j=1}^l \gamma_j \phi(x_j), \quad (23)$$

where $\gamma = (\gamma_1, \dots, \gamma_l)^\top$ is the coefficient vector.

Substituting (23) into (14), we obtain:

$$\min_{\gamma} f(\gamma) = \sum_{i=1}^l \sum_{j=1}^l \frac{1}{2} \gamma_i \gamma_j \mathcal{K}(x_i, x_j) + C \sum_{i=1}^l \frac{1}{\lambda} \left(1 - \frac{1}{1 + \lambda \xi_i^2 e^{a \xi_i}} \right), \quad (24)$$

where $\xi_i = 1 - y_i \left(\sum_{j=1}^l \gamma_j \mathcal{K}(x_j, x_i) \right)$, and $\mathcal{K}(x_j, x_i) = (\phi(x_j) \cdot \phi(x_i))$ is the Kernel function.

In the same way, as in linear Wave-SVM, we use the following formulas to obtain the gradient, exponentially decaying averages of past gradients and past squared gradients, and then update the parameter γ . The Adam algorithm structure for non-linear Wave-SVM is clearly described in Algorithm 1.

$$\nabla f(\gamma_t) = \mathcal{K} \gamma - \sum_{i=1}^k \frac{C y_i \mathcal{K}_i \xi_i (2 + \xi_i) \exp(a \xi_i)}{\left[1 + \lambda \xi_i^2 \exp(a \xi_i) \right]^2}, \quad (26)$$

where \mathcal{K} is the Gaussian Kernel matrix of the randomly selected training dataset and \mathcal{K}_i is the i^{th} row of

Algorithm 1 Non-linear Wave-SVM

Input:

The dataset: $\{x_i, y_i\}_{i=1}^l$, $y_i \in \{-1, 1\}$;

The parameters: Regularization parameter C , wave loss parameters λ and a , mini-batch size k , decay rates β_1 and β_2 , learning rate α , constant ϵ , error tolerance η , maximum iteration number T ;

Initialize: γ_0 and t ;

Output:

The classifiers parameters: γ ;

1 : Select k samples $\{x_i, y_i\}_{i=1}^k$ uniformly at random.

2 : Computing ξ_i :

$$\xi_i = 1 - y_i \left(\sum_{j=1}^k \gamma_j \mathcal{K}(x_j, x_i) \right), \quad i = 1, \dots, k; \quad (25)$$

3 : Compute $\nabla f(\gamma_t)$: (26);

4 : Compute m'_t : (27);

5 : Compute v'_t : (28);

6 : Compute \hat{m}'_t : (29);

7 : Compute \hat{v}'_t : (30);

8 : Update SVM solution γ_t : (31);

9 : Update iteration number: $t = t + 1$.

Until:

$|\gamma_t - \gamma_{t-1}| < \eta$ or $t = T$

Return: γ_t .

the matrix \mathcal{K} .

$$m'_t = \beta_1 m'_{t-1} + (1 - \beta_1) \nabla f(\gamma_t), \quad (27)$$

$$v'_t = \beta_2 v'_{t-1} + (1 - \beta_2) \nabla f(\gamma_t)^2, \quad (28)$$

$$\hat{m}'_t = \frac{m'_t}{(1 - \beta_1)}, \quad (29)$$

$$\hat{v}'_t = \frac{v'_t}{(1 - \beta_2)}. \quad (30)$$

Eventually, the parameter γ is updated as follows:

$$\gamma_t = \gamma_{t-1} - \alpha \frac{\hat{m}'_t}{\sqrt{\hat{v}'_t} + \epsilon}. \quad (31)$$

When the optimal γ is obtained, the following decision function can be utilized to predict the label of a new sample x .

$$\hat{y} = \text{sign}(f(x)) = \text{sign} \left(\sum_{j=1}^k \gamma_j \mathcal{K}(x_j, x) \right). \quad (32)$$

2.4. Formulation of Wave-TSVM

In this subsection, we amalgamate the proposed asymmetric wave loss function into the least squares setting of TSVM and propose a robust and smooth classifier referred to as Wave-TSVM. Let $X_+ = (x_1, \dots, x_{l_+})^\top \in \mathbb{R}^{l_+ \times n}$ and $X_- = (x_1, \dots, x_{l_-})^\top \in \mathbb{R}^{l_- \times n}$ represent matrices containing positive and negative instances, where l_+ and l_- denote the count of positive and negative instances, respectively, and $l = l_+ + l_-$. Further, e_1 and e_2 are identity vectors of appropriate size, and I is the identity matrix of appropriate size.

2.4.1. Linear Wave-TSVM

Given a training dataset \mathcal{D} , the goal of Wave-TSVM is to obtain the positive and negative hyperplanes as follows:

$$w_+^\top x + b_+ = 0 \quad \text{and} \quad w_-^\top x + b_- = 0, \quad (33)$$

where $w_+, w_- \in \mathbb{R}^n$ and $b_+, b_- \in \mathbb{R}$ are the weight vectors and the bias terms, respectively. To obtain the hyperplanes (33), the primal of linear Wave-TSVM are formed as follows:

(Linear Wave-TSVM-1)

$$\begin{aligned} \min_{w_+, b_+, \xi^-} & \frac{1}{2} \sum_{i=1}^{l_+} (w_+^\top x_i + b_+)^2 + \frac{1}{2} C_1 (\|w_+\|_2^2 + b_+^2) + C_2 \sum_{j=1}^{l_-} \xi_j^- \\ \text{s.t. } \xi_j^- &= \frac{1}{\lambda} \left(1 - \frac{1}{1 + \lambda (1 + w_+^\top x_j + b_+)^2 \exp\{a(1 + w_+^\top x_j + b_+)\}} \right), \quad j = 1, \dots, l_-, \end{aligned} \quad (34)$$

(Linear Wave-TSVM-2)

$$\begin{aligned} \min_{w_-, b_-, \xi^+} & \frac{1}{2} \sum_{j=1}^{l_-} (w_-^\top x_j + b_-)^2 + \frac{1}{2} C_3 (\|w_-\|_2^2 + b_-^2) + C_4 \sum_{i=1}^{l_+} \xi_i^+, \\ \text{s.t. } \xi_i^+ &= \frac{1}{\lambda} \left(1 - \frac{1}{1 + \lambda (1 - w_-^\top x_i - b_-)^2 \exp\{a(1 - w_-^\top x_i - b_-)\}} \right), \quad i = 1, \dots, l_+, \end{aligned} \quad (35)$$

where $\xi_+ = (\xi_1^+, \dots, \xi_{l_+}^+)^{\top} \in \mathbb{R}^{l_+}$, $\xi_- = (\xi_1^-, \dots, \xi_{l_-}^-)^{\top} \in \mathbb{R}^{l_-}$. For the sake of brevity, we solely discuss optimization problem (34), noting that optimization problem (35) follows a similar structure. The objective function provided in equation (34) comprises three distinct terms. More precisely, the initial term aims to minimize the distance between the positive hyperplane and the positive instances. The second term, a regularization term, is incorporated to enhance the generalization performance of the model. The third term represents the cumulative penalty of all negative samples, leveraging the proposed wave loss function.

Given the non-convex nature of optimization problems (34) and (35), and utilizing their inherent

smoothness, we devise an iterative algorithm to solve them. Initially, we convert (34) and (35) into vector-matrix form in the following manner:

$$\min_{w_1} P_1(w_1) = \frac{1}{2} \|G^\top w_1\|_2^2 + \frac{1}{2} C_1 \|w_1\|_2^2 + C_2 \mathfrak{L}_1(w_1), \quad (36)$$

and

$$\min_{w_2} P_2(w_2) = \frac{1}{2} \|H^\top w_2\|_2^2 + \frac{1}{2} C_3 \|w_2\|_2^2 + C_4 \mathfrak{L}_2(w_2), \quad (37)$$

where $\mathfrak{L}_1(w_1) = \sum_{j=1}^{l_-} \frac{1}{\lambda} \left(1 - \frac{1}{1 + \lambda (1 + H_j^\top w_1)^2 \exp(a(1 + H_j^\top w_1))} \right)$, $j = 1, \dots, l_-$; $\mathfrak{L}_2(w_2) = \sum_{i=1}^{l_+} \frac{1}{\lambda} \left(1 - \frac{1}{1 + \lambda (1 - G_i^\top w_2)^2 \exp(a(1 - G_i^\top w_2))} \right)$, $i = 1, \dots, l_+$. G_i is the i^{th} column of matrix G and H_j is the j^{th} column of matrix H . $G = [X_+, e_1]^\top \in \mathbb{R}^{(n+1) \times l_+}$, $H = [X_-, e_2]^\top \in \mathbb{R}^{(n+1) \times l_-}$; $w_1 = [w_+^\top, b_+]^\top \in \mathbb{R}^{n+1}$, $w_2 = [w_-^\top, b_-]^\top \in \mathbb{R}^{n+1}$. Further, for simplification, we use A_j and B_i to represent $(1 + H_j^\top w_1)$ and $(1 - G_i^\top w_2)$, respectively.

In accordance with the optimality condition, we obtain the following:

$$\nabla P_1(w_1) = (GG^\top + C_1 I)w_1 + \hat{H}s_1 = 0, \quad (38)$$

$$\nabla P_2(w_2) = (HH^\top + C_3 I)w_2 - \hat{G}s_2 = 0, \quad (39)$$

where $\hat{G} = [C_4 G_1, \dots, C_4 G_{l_+}] \in \mathbb{R}^{(n+1) \times l_+}$, $\hat{H} = [C_2 H_1, \dots, C_2 H_{l_-}] \in \mathbb{R}^{(n+1) \times l_-}$. $s_1 = [s_{11}, \dots, s_{1l_-}]^\top \in \mathbb{R}^{l_-}$, $s_2 = [s_{21}, \dots, s_{2l_+}]^\top \in \mathbb{R}^{l_+}$; $s_{1j} = \frac{A_j(aA_j+2)\exp(aA_j)}{(1+\lambda A_j^2 \exp(aA_j))^2}$, $j = 1, \dots, l_-$; $s_{2i} = \frac{B_i(aB_i+2)\exp(aB_i)}{(1+\lambda B_i^2 \exp(aB_i))^2}$, $i = 1, \dots, l_+$.

Now, we use equations (38) and (39) to formulate iterative equations for optimization problems (36) and (37) in the following manner:

$$w_1^{t+1} = - (GG^\top + C_1 I)^{-1} \hat{H}s_1^t, \quad (40)$$

$$w_2^{t+1} = (HH^\top + C_3 I)^{-1} \hat{G}s_2^t. \quad (41)$$

Here, t represents the number of iteration. The iterative procedure involves iterating through equations (40) and (41) until convergence is achieved. After obtaining the solutions, we can proceed to find the pair of hyperplanes (33).

To ascertain the class of a unseen sample $\tilde{x} \in \mathbb{R}^n$, we use the following decision rule:

$$\text{Class of } \tilde{x} = \begin{cases} +1, & \text{if } \frac{|w_+^\top \tilde{x} + b_+|}{\|w_+\|} \leq \frac{|w_-^\top \tilde{x} + b_-|}{\|w_-\|}, \\ -1, & \text{otherwise.} \end{cases} \quad (42)$$

2.4.2. Non-linear Wave-TSVM

In the case of non-linearity, data points are separated linearly in a higher-dimensional feature space by utilizing the kernel trick to map them to a higher feature space. The objective of non-linear Wave-TSVM is to identify a pair of hypersurfaces in the following manner:

$$\mathcal{K}(x, X^\top) v_+ + b_+ = 0 \quad \text{and} \quad \mathcal{K}(x, X^\top) v_- + b_- = 0, \quad (43)$$

where $X = [X_+; X_-]^\top$ and $\mathcal{K}(\cdot, \cdot)$ is the kernel function. To determine the hypersurfaces (43), we formulate the following optimization problems:

(Non-linear Wave-TSVM-1)

$$\begin{aligned} & \min_{v_+, b_+, \zeta^-} \sum_{i=1}^{l_+} \frac{1}{2} (\mathcal{K}(x_i, X^\top) v_+ + b_+)^2 + \frac{1}{2} C_1 (\|v_+\|_2^2 + b_+^2) + C_2 \sum_{j=1}^{l_-} \zeta_j^-, \\ \text{s.t.} \quad & \zeta_j^- = \frac{1}{\lambda} \left(1 - \frac{1}{1 + \lambda (1 + \mathcal{K}(x_j, X^\top) v_+ + b_+)^2 \exp\{a (1 + \mathcal{K}(x_j, X^\top) v_+ + b_+)\}} \right), \\ & j = 1, \dots, l_-, \end{aligned} \quad (44)$$

(Non-linear Wave-TSVM-2)

$$\begin{aligned} & \min_{v_-, b_-, \zeta^+} \sum_{j=1}^{l_-} \frac{1}{2} (\mathcal{K}(x_j, X^\top) v_- + b_-)^2 + \frac{1}{2} C_3 (\|v_-\|_2^2 + b_-^2) + C_4 \sum_{i=1}^{l_+} \zeta_i^+, \\ \text{s.t.} \quad & \zeta_i^+ = \frac{1}{\lambda} \left(1 - \frac{1}{1 + \lambda (1 - \mathcal{K}(x_i, X^\top) v_- - b_-)^2 \exp\{a (1 - \mathcal{K}(x_i, X^\top) v_- - b_-)\}} \right), \\ & i = 1, \dots, l_+. \end{aligned} \quad (45)$$

The method for solving problems (44) and (45) is akin to the linear scenario. The iterative method corresponds to equations (44) and (45) can be derived as follows:

$$\begin{aligned} v_1^{t+1} &= - \left(M M^\top + C_1 I \right)^{-1} \\ & \left(\sum_{j=1}^{l_-} C_2 N_j \frac{(1 + N_j^\top v_1^t)(a(1 + N_j^\top v_1^t) + 2) \exp(a(1 + N_j^\top v_1^t))}{\{1 + \lambda(1 + N_j^\top v_1^t)^2 \exp(a(1 + N_j^\top v_1^t))\}^2} \right), \end{aligned} \quad (46)$$

$$\begin{aligned} v_2^{t+1} &= \left(N N^\top + C_3 I \right)^{-1} \\ & \left(\sum_{i=1}^{l_+} C_4 M_i \frac{(1 - M_i^\top v_2^t)(a(1 - M_i^\top v_2^t) + 2) \exp(a(1 - M_i^\top v_2^t))}{\{1 + \lambda(1 - M_i^\top v_2^t)^2 \exp(a(1 - M_i^\top v_2^t))\}^2} \right). \end{aligned} \quad (47)$$

Here $M = [\mathcal{K}(X_+, X^\top), e_1]^\top \in \mathbb{R}^{(l+1) \times l_+}$, $N = [\mathcal{K}(X_-, X^\top), e_2]^\top \in \mathbb{R}^{(l+1) \times l_-}$; M_i is the i^{th} column of the matrix M , N_j is the j^{th} column of the matrix N . $v_1 = [v_+^\top, b_+]^\top$, $v_2 = [v_-^\top, b_-]^\top$. Further, for simplification, we use E_j and F_i to represent $(1 + N_j^\top v_1)$ and $(1 - M_i^\top v_2)$, respectively.

It's important to highlight that equations (46) and (47) entail the intricate calculation of matrix inversion. Therefore, we utilized the Sherman-Morrison-Woodbury (SMW) theorem [31] to alleviate computational complexity. Subsequently, in equations (46) and (47), the inverse matrices are substituted with the following matrices:

$$Q_1 = \frac{1}{C_1} \left(I - M \left(C_1 I + M^\top M \right)^{-1} M^\top \right), \quad (48)$$

$$Q_2 = \frac{1}{C_3} \left(I - N \left(C_3 I + N^\top N \right)^{-1} N^\top \right). \quad (49)$$

Using the equations (48) and (49), the iterative approach can be derived in the following manner:

$$v_1^{t+1} = -Q_1 \hat{N} s_1^t, \quad (50)$$

$$v_2^{t+1} = Q_2 \hat{M} s_2^t, \quad (51)$$

where t denotes the number of iteration. Also, $\hat{N} = [C_2 N_1, \dots, C_2 N_{l_-}] \in \mathbb{R}^{(l+1) \times l_-}$, and $\hat{M} = [C_4 M_1, \dots, C_4 M_{l_+}] \in \mathbb{R}^{(l+1) \times l_+}$. Additionally, $s_1^t \in \mathbb{R}^{l_-}$, $s_{1j}^t = \frac{E_j'(aF_j'+2)\exp(aE_j')}{\{1+\lambda E_j'^2 \exp(aE_j')\}^2}$, $j = 1, \dots, l_-$; $s_2^t \in \mathbb{R}^{l_+}$, $s_{2i}^t = \frac{F_i'(aF_i'+2)\exp(aF_i')}{\{1+\lambda F_i'^2 \exp(aF_i')\}^2}$, $i = 1, \dots, l_+$. The iterative procedure can be established by iterating through equations (50) and (51) until convergence is achieved. Consequently, upon obtaining the solutions v_+, b_+ and v_-, b_- , we can then determine the positive and negative hypersurfaces generated by the kernel.

For a new sample $\tilde{x} \in \mathbb{R}^n$, we use the following decision function:

$$\text{Class of } \tilde{x} = \begin{cases} +1, & \text{if } \frac{|\mathcal{K}(\tilde{x}, X^\top)v_+ + b_+|}{\sqrt{v_+^\top \mathcal{K}(X, X^\top)v_+}} \leq \frac{|\mathcal{K}(\tilde{x}, X^\top)v_- + b_-|}{\sqrt{v_-^\top \mathcal{K}(X, X^\top)v_-}}, \\ -1, & \text{otherwise.} \end{cases} \quad (52)$$

The iterative algorithm structure for non-linear Wave-TSVM subproblem (44) is clearly described in Algorithm 2. The structure for subproblem (45) is similar to it.

2.5. Computational Complexity

In this subsection, we discuss the computational complexity of the proposed Wave-SVM and Wave-TSVM. Let l and n denote the number of samples and features in training dataset, respectively, and k denote the size of the mini-batch. The l_+ and l_- denote the count of positive and negative samples, respectively. The

Algorithm 2 Non-linear Wave-TSVM

Input:

 Training dataset: $\{x_i, y_i\}_{i=1}^l$, $y_i \in \{-1, 1\}$;

 The parameters: Convergence precision (η), maximum iteration number (T), parameter C_1 and C_2 , wave loss parameters a and λ , iteration number $t = 0$;

 Initialize: v_1^0 ;

Ensure: v_+ , b_+ ;

 1 : $M = [\mathcal{K}(X_+, X^\top), e_1]^\top$, $N = [\mathcal{K}(X_-, X^\top), e_2]^\top$.

 2 : **while** $t \leq T$ **do**

 3 : **for** $j \leftarrow 1$ to l_- **do**

 4 : $s_{1j}^t \leftarrow \frac{E_j^t(aE_j^t+2)\exp(aE_j^t)}{(1+\lambda E_j^t)^2 \exp(aE_j^t))^2}$.

 5 : **end for**

 6 : $v_1^{t+1} \leftarrow -Q_1 \hat{N} s_1^t$

 7 : **if** $\|v_1^{t+1} - v_1^t\| < \eta$ **then**

8 : break

 9 : **else**

 10 : $t \leftarrow t + 1$

 11 : **end if**

 12 : **end while**

 13 : $(v_+^\top, b_+^\top)^\top = v_1^{t+1}$.

computational complexity of Wave-SVM is dominated by the computation of the gradients, characterized by a complexity of $O(k^2)$. Further, the process of computing the moving averages of the gradients' first and second moments, as well as performing bias correction for these averages, both require $O(k)$ operations, as we have k model parameter to compute. Therefore, the overall computational complexity of the Wave-SVM can be considered as $O(T(k^2+k))$, where T represents the maximum number of iterations. This encapsulates the fundamental operations involved in training the Wave-SVM and underscores its scalability concerning the number of iterations and features. The computational complexity of Wave-TSVM primarily arises from the computation of matrix inversion. In the linear case, the algorithm requires solving the inverse of a $(n+1) \times (n+1)$ matrix, which results in a time complexity of $O((n+1)^3)$. For the non-linear case, the algorithm needs to compute the inverse of two matrices: one of size $l_+ \times l_+$ and the other of size $l_- \times l_-$, with computational complexities of $O(l_+^3)$ and $O(l_-^3)$, respectively. Hence, for non-linear Wave-TSVM, the time complexity is $O(T(l_+^3 + l_-^3))$. It is evident that non-linear Wave-TSVM is not well-suited for large-scale datasets due to its cubic computational complexity growth in relation to the sample size.

3. Numerical Experiments

In this section, we assess the proposed Wave-SVM and Wave-TSVM against the baseline models, including C-SVM [2], Pin-SVM [11], LINEX-SVM [18], FP-SVM [15], TSVM [7], Pin-GTSVM [32], SLTSVM [33], and IF-RVFL [34]. For experiments, we downloaded 42 binary datasets of diverse domains

from the UCI [35] and KEEL [36] repositories. The detailed description of the datasets is provided in Table S.I of the supplementary file. Additionally, we assess the models on the Alzheimer’s disease (AD) dataset, available on the Alzheimer’s Disease Neuroimaging Initiative (ADNI) (adni.loni.usc.edu).

3.1. Experimental Setup and Parameter Selection

All the experiments are implemented using MATLAB R2023a on window 10 running on a PC with configuration Intel(R) Core(TM) i7-6700 CPU @ 3.40GHz, 3408 Mhz, 4 Core(s), 8 Logical Processor(s) with 16 GB of RAM. For each SVM type model (C-SVM [2], Pin-SVM [11], LINEX-SVM [18], FP-SVM [15], and proposed Wave-SVM), the regularization parameter C is selected from the set $\{10^i | i = -6, -5, \dots, 5, 6\}$. For Pin-SVM, the hyperparameter τ is chosen from the set $\{0, 0.1, \dots, 0.9, 1\}$. For LINEX-SVM and FP-SVM, the loss hyperparameters are selected the same as in [18] and [15], respectively. For the proposed Wave-SVM, loss hyperparameters λ and a are selected from the ranges $[0.1 : 0.2 : 2]$ and $[-2 : 0.1 : 5]$, respectively. For the non-linear case, Gaussian kernel function $\mathcal{K}(x_j, x_k) = \exp(-\|x_j - x_k\|^2 / \sigma^2)$ (where σ is the kernel parameter) is considered. The Gaussian kernel parameter σ for each SVM type model is selected from the set $\{10^i | i = -6, -5, \dots, 5, 6\}$. The parameters for the Adam algorithm are experimentally set as: (i) initial weight $w_0 = 0.01$, (ii) initial first moment $m_0 = 0.01$, (iii) initial second moment $v_0 = 0.01$, (iv) initial learning rate α is selected from the set $\{0.0001, 0.001, 0.01\}$, (v) exponential decay rate of first order $\beta_1 = 0.9$, (vi) exponential decay rate of second order $\beta_2 = 0.999$, (vii) error tolerance $\eta = 10^{-5}$, (viii) division constant $\epsilon = 10^{-8}$, (ix) mini-batch size $k = 2^5$, (x) maximum iteration number $T = 1000$.

For each TSVM type model (TSVM [7], Pin-GTSVM [32], SLTSVM [33], and proposed Wave-TSVM), the regularization parameters (C_1 and C_3) and kernel parameter (σ) are selected from the set $\{10^i | i = -6, -4, \dots, 4, 6\}$. For Pin-GTSVM, the hyperparameter τ is selected the same as in [32]. For SLTSVM and the proposed Wave-TSVM, the structural risk minimization parameters C_2 and C_4 are selected from the set $\{10^i | i = -6, -4, \dots, 4, 6\}$. For SLTSVM and the proposed Wave-TSVM, we set $C_1 = C_3$ and $C_2 = C_4$. For iterative algorithm, to solve SLTSVM and the proposed Wave-TSVM, we set $\eta = 10^{-5}$ and $T = 50$. To suppress the tuning time for the proposed Wave-TSVM on UCI and KEEL datasets, the loss hyperparameter λ is fixed to 1, and a is selected from the range $[-2 : 0.5 : 2]$. For IF-RVFL [34], the regularization parameter (C) and kernel parameter (σ) are selected from the set $\{10^i | i = -6, -4, \dots, 4, 6\}$, and the number of hidden nodes (N_d) is selected from the range $[3 : 20 : 203]$ [37].

The performance of the models significantly depends on the selection of parameters [38]. In order to adjust them, we tune the parameters based on k-fold (k= 4) cross-validation and grid search. The benefit behind k-fold cross-validation is that it ensures that every sample will eventually be included in both the

training and testing sets. More specifically, the dataset is divided into four non-overlapping subsets at random, one of which is set aside as a test set and the other three as train set. This process is conducted four times, and at every setup, a different test set is chosen while the other three sets are used as training, and the best of the four testing results is used as the performance measure for each model. For all the experiments, we normalized the data in the range of $[0, 1]$.

To assess the efficacy of the proposed Wave-SVM and Wave-TSVM against baseline models, we employed the accuracy metric, defined as follows:

$$\text{Accuracy} = \frac{\text{T.P.} + \text{T.N.}}{\text{T.P.} + \text{T.N.} + \text{F.P.} + \text{F.N.}} \times 100. \quad (53)$$

Here, T.P., T.N., F.P., and F.N. represent the true positive, true negative, false positive, and false negative, respectively. Further, we conducted a comparative analysis of the training time between the proposed Wave-SVM and the baseline models. The reported times only include the time taken for training the models with the optimized hyperparameters.

3.2. Evaluation on UCI and KEEL datasets

For a fair comparison of the proposed Wave-SVM and Wave-TSVM with baseline models, we compare Wave-SVM with C-SVM, Pin-SVM, LINEX-SVM, and FP-SVM, and Wave-TSVM with TSVM, Pin-GTSVM, and SLTSVM. In essence, we compared Wave-SVM and Wave-TSVM with SVM type models and TSVM type models, respectively. Additionally, we compare Wave-TSVM with IF-RVFL.

First, we discuss the experimental outcomes of Wave-SVM. For linear case, the average classification accuracy and training time of the proposed Wave-SVM and the baseline models (C-SVM, Pin-SVM, LINEX-SVM, and FP-SVM) are presented in Table 2. The detailed experimental results for each dataset are presented in Table S.VI of the supplementary file. The average accuracy of the existing C-SVM, Pin-SVM, LINEX-SVM, and FP-SVM are 82.21%, 89.1%, 77.41%, and 89.73% respectively, whereas, the average accuracy of the proposed Wave-SVM is 91.15%, surpassing the baseline models. The average training time, expressed in seconds, of C-SVM, Pin-SVM, LINEX-SVM, FP-SVM, and the proposed Wave-SVM are 4.6266s, 7.074s, 0.0033s, 2.254, and 0.0049s, respectively. This observation strongly underscores the substantial superiority of the proposed Wave-SVM over C-SVM and Pin-SVM. However, its training time is marginally extended compared to LINEX-SVM. Nonetheless, it still demonstrates commendable performance in terms of training time. The optimal parameters of linear Wave-SVM and baseline models corresponding to the accuracy values are presented in Table S.VII of the supplementary file. For the non-linear case, the average accuracy and training time of the proposed Wave-SVM and baseline models are

presented in Table 3. The detailed experimental results of non-linear Wave-SVM against baseline models for each dataset are presented in Table S.VIII of the supplementary file. The average accuracy of C-SVM, Pin-SVM, LINEX-SVM, FP-SVM, and the proposed Wave-SVM are 89.46%, 89.97%, 86.63%, 90.18%, and 91.92%, respectively. Evidently, the proposed Wave-SVM achieves the highest classification accuracy in comparison with the baseline models. The average training time of C-SVM, Pin-SVM, LINEX-SVM, FP-SVM, and the proposed Wave-SVM are 7.57s, 8.64s, 0.0137s, 1.39s, and 0.0219s, respectively. The outcomes manifest that the proposed Wave-SVM exhibits remarkable efficiency. Its training time is significantly less than C-SVM and Pin-SVM, indicating its enhanced computational efficiency. However, the proposed Wave-SVM takes a slightly longer time to train than the LINEX-SVM, although the difference in training time is minor. It is noteworthy that the comparative evaluation of accuracy and training time shows the overall performance of the models. Thus, the proposed Wave-SVM's ability to strike a balance between classification accuracy and training time makes it a superior model in comparison to the baseline models. The optimal parameters of non-linear Wave-SVM and baseline models corresponding to the accuracy values are presented in Table S.IX of the supplementary file.

To assess the TSVM type models, given the substantial computational complexity of the proposed Wave-TSVM due to the matrix inversion, we excluded datasets with either over 5000 samples or more than 25 features. This exclusion resulted in a remaining set of 32 datasets. The average experimental outcomes for the non-linear proposed Wave-TSVM and baseline models, including TSVM, Pin-GTSVM, SLTSVM, and IF-RVFL, across these 32 datasets are presented in Table 4. For detailed results on each dataset, refer to Table S.X of the supplementary file. The average classification accuracies of the existing TSVM, Pin-GTSVM, IF-RVFL, and SLTSVM are 86.49%, 83.24%, 83.8%, and 85.98%, respectively. In contrast, the average accuracy of the proposed Wave-TSVM is 87.91%, surpassing that of baseline models. These findings strongly emphasize the significant superiority of the proposed Wave-TSVM over the baseline models. The optimal parameters of non-linear Wave-TSVM and baseline models corresponding to the accuracy values are outlined in Table S.XI of the supplementary file.

Further, to offer additional substantiation for the enhanced efficacy of the proposed Wave-SVM and Wave-TSVM, we conducted a thorough statistical analysis of the models, for which we followed four tests: ranking scheme, Friedman test, Nemenyi post hoc test, and Win-Tie-Loss sign test. A detailed discussion of the statistical tests and their results is presented in Section S.II of the supplementary file.

3.3. Evaluation on UCI and KEEL datasets with Gaussian noise

While the UCI and KEEL datasets used in our evaluation reflect real-world circumstances, it is essential to acknowledge that outliers or noise can arise due to various factors. To showcase the effectiveness of the

Table 2: Average accuracy, training time and rank for linear Wave-SVM against baseline models on benchmark UCI and KEEL datasets.

Dataset	C-SVM [2]	Pin-SVM [11]	LINEX-SVM [18]	FP-SVM [15]	Wave-SVM [†]
Avg. Acc.	82.21	89.1	77.41	89.73	91.15
Avg. Time	4.6266	7.074	0.0033	2.254	0.0049
Avg. Rank	3.73	2.52	4.29	2.49	1.68

[†] represents the proposed model.

Here, Avg. and Acc. are acronyms used for average and accuracy, respectively.

Table 3: Average accuracy, training time and rank for non-linear Wave-SVM against baseline models using Gaussian kernel function on benchmark UCI and KEEL datasets.

Dataset	C-SVM [2]	Pin-SVM [11]	LINEX-SVM [18]	FP-SVM [15]	Wave-SVM [†]
Avg. Acc.	89.46	89.97	86.63	90.18	91.92
Avg. Time	7.57	8.64	0.0137	1.39	0.0219
Avg. Rank	3.37	2.85	4.16	2.53	1.8

[†] represents the proposed model.

Here, Avg. and Acc. are acronyms used for average and accuracy, respectively.

proposed Wave-SVM and Wave-TSVM, even in adverse conditions, we deliberately added feature noise to selected datasets. We selected 6 diverse datasets for our comparative analysis, namely breast_cancer_wisc, credit_approval, horse_colic, led7digit-0-2-4-5-6-7-8-9_vs_1, monk1, and yeast2vs8. To ensure impartiality in evaluating the models, we selected 2 datasets where the proposed Wave-SVM achieves the highest performance compared to baseline models at 0% noise level (refer to Table S.VIII of supplementary). Further, we selected 2 datasets where the proposed Wave-SVM does not achieve the highest performance and 2 datasets where the proposed Wave-SVM ties with an existing model. To carry out a comprehensive evaluation, we added Gaussian noise at varying levels of 5%, 10%, 20%, and 30% to corrupt the features of these datasets. The accuracy values of Wave-SVM against baseline models for the selected datasets with 5%, 10%, 20%, and 30% level of noise are presented in Table 5. Out of 6 diverse datasets, the proposed Wave-SVM outperforms the baseline models on 5 datasets and attains second position on 1 dataset, as per the average accuracies at different levels of noise. This outcome unequivocally underscores the significance of the proposed Wave-SVM as a robust model. The optimal parameters of Wave-SVM and baseline models corresponding to the accuracy values on noisy datasets are presented in Table S.IX of the supplementary. Similarly, the accuracy values of Wave-TSVM against baseline models for the selected datasets with 5%, 10%, 20%, and 30% noise levels are outlined in Table 6. Out of the 6 diverse datasets, the proposed Wave-TSVM surpasses the baseline algorithms on 4 datasets, achieves the second position on 1 dataset, and secures the third position on 1 dataset, based on the average accuracies at different noise levels. This result demonstrate the significance and robustness of Wave-TSVM. The optimal parameters of Wave-TSVM and baseline models corresponding to the accuracy values on noisy datasets are presented

Table 4: Average accuracy and rank for non-linear Wave-TSVM against baseline models on benchmark UCI and KEEL datasets.

Dataset	TSVM [7]	Pin-GTSVM [32]	IF-RVFL [34]	SLSTSVM [33]	Wave-TSVM [†]
Avg. Acc.	86.49	83.24	83.8	85.98	87.91
Avg. Rank	2.78	3.55	3.75	2.92	2

[†] represents the proposed model.

Here, Avg. and Acc. are acronyms used for average and accuracy, respectively.

Table 5: Performance comparison of the proposed Wave-SVM compare baseline models on benchmark UCI and KEEL datasets with Gaussian noise.

Model	C-SVM [2]	Pin-SVM [11]	LINEX-SVM [18]	FP-SVM [15]	Wave-SVM [†]
Dataset	Noise	Accuracy	Accuracy	Accuracy	Accuracy
breast_cancer_wisc	5%	93.68	97.7	100	100
	10%	94.25	97.7	100	100
	20%	87.36	97.7	100	100
	30%	85.14	98.85	100	100
	Avg. Acc.	90.11	97.99	100	100
credit_approval	5%	85.55	84.88	91.33	94.8
	10%	86.13	85.47	89.02	95.38
	20%	84.97	86.13	89.02	95.38
	30%	84.39	84.97	89.02	92.49
	Avg. Acc.	85.26	85.36	89.6	95.09
horse_colic	5%	70.65	76.09	81.52	85.87
	10%	70.65	73.91	82.61	84.78
	20%	69.57	71.74	80.43	88.04
	30%	68.48	69.57	80.43	86.96
	Avg. Acc.	69.84	72.83	<u>81.25</u>	86.41
led7digit-0-2-4-5-6-7-8-9_vs_1	5%	96.4	96.4	96.4	97.3
	10%	96.4	96.4	93.69	98.2
	20%	96.4	96.4	95.45	97.3
	30%	96.36	96.4	94.59	97.3
	Avg. Acc.	96.39	96.4	95.03	<u>97.52</u>
monk1	5%	56.12	53.96	56.83	59.71
	10%	54.68	57.55	53.96	58.27
	20%	55.4	56.83	56.12	58.27
	30%	58.27	56.83	56.83	61.87
	Avg. Acc.	56.12	56.29	55.93	<u>59.53</u>
yeast2vs8	5%	98.35	98.35	98.35	99.17
	10%	98.35	98.35	98.35	99.17
	20%	98.35	98.35	98.35	99.17
	30%	98.35	98.35	98.35	100
	Avg. Acc.	98.35	98.35	98.35	<u>99.17</u>

[†] represents the proposed model.

Here, Avg. and Acc. are acronyms used for average and accuracy, respectively.

The boldface and underline indicate the best and second-best models, respectively, in terms of average accuracy.

in Table S.XI of the supplementary. By subjecting the models to rigorous conditions, we demonstrate the exceptional performance and superiority of the proposed Wave-SVM and Wave-TSVM, especially in adverse scenarios.

Table 6: Performance comparison of the proposed Wave-TSVM compare baseline models on benchmark UCI and KEEL datasets with Gaussian noise.

Model	TSVM [7]	Pin-GTSVM [32]	IF-RVFL [34]	SLSTSVM [33]	Wave-TSVM [†]
Dataset	Noise	Accuracy	Accuracy	Accuracy	Accuracy
breast_cancer_wisc	5%	88.01	88.68	83.57	78.16
	10%	88.01	88.68	83.57	78.16
	20%	86.9	87.37	83.57	78.16
	30%	84.37	85.5	83.57	78.16
	Avg. Acc.	<u>86.82</u>	87.56	83.57	78.16
credit_approval	5%	91.84	90.18	80.92	80.92
	10%	89.53	87.57	80.92	80.81
	20%	86.37	87.57	80.92	79.65
	30%	85.95	84.08	80.92	73.41
	Avg. Acc.	<u>88.42</u>	87.35	80.92	78.7
horse_colic	5%	75.04	82.25	77.61	75
	10%	75.04	79.9	77.61	71.74
	20%	73.22	79.9	77.61	70.65
	30%	69.04	68.86	77.61	72.83
	Avg. Acc.	73.1	<u>77.73</u>	77.61	72.55
led7digit-0-2-4-5-6-7-8-9_vs_1	5%	95.3	93.81	89.37	95.5
	10%	95.3	87.09	89.37	95.5
	20%	93.5	87.09	89.37	93.69
	30%	91.4	84.5	89.37	93.69
	Avg. Acc.	93.87	88.12	89.37	<u>94.6</u>
monk1	5%	55.71	52.15	61.15	61.15
	10%	56.99	52.15	61.15	60.43
	20%	58.15	53.98	61.15	57.55
	30%	59.71	51.18	61.15	61.15
	Avg. Acc.	57.64	<u>52.37</u>	61.15	<u>60.07</u>
yeast2vs8	5%	99.17	88.55	89.92	97.52
	10%	98.35	88.55	89.92	98.35
	20%	97.69	88.55	89.92	98.35
	30%	96.04	88.1	89.92	97.52
	Avg. Acc.	97.81	88.44	89.92	<u>97.93</u>

[†] represents the proposed model.

Here, Avg. and Acc. are acronyms used for average and accuracy, respectively.

The boldface and underline indicate the best and second-best models, respectively, in terms of average accuracy.

3.4. Results Analysis on ADNI dataset

Alzheimer’s disease (AD) is a widely recognized neurodegenerative illness that progressively results in memory loss and cognitive impairments. AD development is irreversible and manifests as atrophy in the brain’s inner regions. It is predicted that by the year 2050, one out of every 85 individuals will suffer from AD [39]. Multiple studies indicate that early detection and intervention can slow down the progression of AD. Therefore, to mitigate further growth, treatment should commence at the earliest possible stage. The ADNI project, initiated by Michael W. Weiner in 2003, aims to examine various neuroimaging techniques, including positron emission tomography (PET), magnetic resonance imaging (MRI), and other diagnostic tests for AD, particularly at the mild cognitive impairment (MCI) stage. AD data is publicly available on

the ADNI repository, which is accessible at adni.loni.usc.edu. The pipeline for feature extraction opted in this paper is the same as followed in [40]. The dataset contains three cases: control normal (CN) versus AD, CN versus MCI, and MCI versus AD.

The accuracy of the proposed Wave-SVM, as well as baseline models for AD diagnosis, are presented in Table 7. We examine that with an average accuracy of 79.11%, the proposed Wave-SVM is the best model. The average accuracies of baseline algorithms, C-SVM, Pin-SVM, and LINEX-SVM are 70.55%, 78.16%, and 75.99%, respectively. With an accuracy of 88.46% and 79.45%, the proposed Wave-SVM is the most accurate classifier for CN versus AD and MCI versus AD cases. For CN versus MCI case, Pin-SVM came out on top followed by the proposed Wave-SVM. Overall, the proposed Wave-SVM has emerged as the best classifier in comparison to the baseline models for AD diagnosis.

Table 7: Results of the proposed non-linear Wave-SVM against baseline models on ADNI dataset.

Model Dataset (# of samples, # of features)	C-SVM [2] (C, σ)		Pin-SVM [11] (τ, C, σ)		LINEX-SVM [18] (a, C, σ)		FP-SVM [15] ($C, \sigma, \tau_1, \tau_2$)		Wave-SVM [†] (λ, a, C, σ)	
CN versus AD (415, 91)	82.26 1,1	0.0206	84.61 0,0,1,0,001	0.006	86.54 -1,0,001,1	0.0011	84.62 0,000001, 0,000001, 0,5, 0	0.0668	88.46 0,1,-0,6,1000,10	0.0019
CN versus MCI (626, 91)	63.1 10,1	0.0247	74.52 0,2,0,1,0,001	0.0119	68.15 -1,1000,10	0.0018	75.15 0,0001, 0,01, 0, 0,4	0.0241	69.43 0,7,3,2,0,001,10	0.0027
MCI versus AD (585, 91)	66.28 1,1	0.0176	75.34 0,10,0,01	0.0502	73.29 -1,0,001,1	0.0014	73.97 1000000, 0,000001, 0, 0,8	0.0444	79.45 0,1,0,3,100,10	0.0024
Avg. Acc. and Avg. Time	70.55	0.021	78.16	0.0227	75.99	0.0014	77.91	0.0451	79.11	0.0023

[†]represents the proposed model.

Here, Avg. and Acc. are acronyms used for average and accuracy, respectively.

4. Conclusions and Future work

In this paper, we have emphasized the pivotal role of the loss function within the realm of supervised learning, highlighting how the choice of the appropriate loss function significantly influences the proficiency of the developed models. We introduced an innovative asymmetric loss function named wave loss. This novel loss function is distinguished by its aptitude for handling outliers, resilience against noise, bounded characteristics, and an essential smoothness property. These distinctive attributes collectively position the wave loss function to effectively address the complex challenges posed by real-world data. Further, by showing the possession of classification-calibrated property, we have laid the foundation for its broader adoption in real-world applications. Additionally, the amalgamation of the proposed wave loss into the least squares setting of SVM and TSVM led to the development of two innovative models: Wave-SVM and Wave-TSVM, respectively. These models offer a robust and smooth alternative to existing classifiers, contributing to the advancement of classification techniques. Notably, the incorporation of the Adam algorithm for optimizing the Wave-SVM brings further innovation, as this is the first time that Adam has been utilized to solve an SVM model. This strategic use of Adam not only improves the efficiency of Wave-SVM but also offers a solution for handling large-scale problems. To tackle the optimization problem of

Wave-TSVM, we utilize an iterative algorithm that requires matrix inversion at each iteration, which is intractable for large datasets. In the future, one can reformulate the Wave-TSVM to circumvent the need to compute matrix inversion. The empirical results garnered from a diverse spectrum of UCI and KEEL datasets (with and without feature noise) undeniably affirm the efficacy of the proposed Wave-SVM and Wave-TSVM against baseline algorithms.

However, we did not explore the application of the wave loss function within deep learning models, which presents an avenue for future research. Looking ahead, the crucial smoothness property inherent to the wave loss function suggests promising possibilities for its fusion with advanced machine learning and deep learning techniques. In future, researchers can explore the fusion of the wave loss function with cutting-edge methodologies like support matrix machines to tackle complex real-world problems. The source codes of the proposed models are publicly available at <https://github.com/mtanveer1/Wave-SVM>.

Acknowledgment

This project is supported by the Indian government’s Science and Engineering Research Board (MTR/2021/000787) under the Mathematical Research Impact-Centric Support (MATRICS) scheme. The Council of Scientific and Industrial Research (CSIR), New Delhi, provided a fellowship for Mushir Akhtar’s research under grant no. 09/1022(13849)/2022-EMR-I. The collection and sharing of data for this project were supported by funding from the Alzheimer’s Disease Neuroimaging Initiative (ADNI) through the National Institutes of Health Grant U01 AG024904 and the DOD ADNI through the Department of Defense award number W81XWH-12-2-0012. ADNI receives funding from the National Institute on Aging, the National Institute of Biomedical Imaging and Bioengineering, and generous contributions from the following sources: AbbVie, Alzheimer’s Association; Alzheimer’s Drug Discovery Foundation; Araclon Biotech; BioClinica, Inc.; Biogen; Bristol-Myers Squibb Company; CereSpir, Inc.; Cogstate; Eisai Inc.; Elan Pharmaceuticals, Inc.; Eli Lilly and Company; EuroImmun; F. Hoffmann-La Roche Ltd and its affiliated company Genentech, Inc.; Fujirebio; GE Healthcare; IXICO Ltd.; Janssen Alzheimer Immunotherapy Research & Development, LLC.; Johnson & Johnson Pharmaceutical Research & Development LLC.; Lumosity; Lundbeck; Merck & Co., Inc.; Meso Scale Diagnostics, LLC.; NeuroRx Research; Neurotrack Technologies; Novartis Pharmaceuticals Corporation; Pfizer Inc.; Piramal Imaging; Servier; Takeda Pharmaceutical Company; and Transition Therapeutics. The Canadian Institutes of Health Research is funding ADNI clinical sites in Canada. Private sector donations are managed by the Foundation for the National Institutes of Health (www.fnih.org). The Northern California Institute for Research and Education is the

grantee organization, and the study is coordinated by the Alzheimer’s Therapeutic Research Institute at the University of Southern California. ADNI data are distributed by the Laboratory for Neuro Imaging at the University of Southern California.

References

- [1] Qi Wang, Yue Ma, Kun Zhao, and Yingjie Tian. A comprehensive survey of loss functions in machine learning. *Annals of Data Science*, pages 1–26, 2020.
- [2] Corinna Cortes and Vladimir Vapnik. Support-vector networks. *Machine Learning*, 20(3):273–297, 1995.
- [3] Xiangmin Han, Jun Wang, Shihui Ying, Jun Shi, and Dinggang Shen. ML-DSVM+: A meta-learning based deep SVM+ for computer-aided diagnosis. *Pattern Recognition*, 134:109076, 2023.
- [4] Haize Hu, Yunyi Li, Xiangping Zhang, and Mengge Fang. A novel hybrid model for short-term prediction of wind speed. *Pattern Recognition*, 127:108623, 2022.
- [5] Eric Lopez-Lopez, Xose M Pardo, and Carlos V Regueiro. Incremental learning from low-labelled stream data in open-set video face recognition. *Pattern Recognition*, 131:108885, 2022.
- [6] Xiao-Xiao Niu and Ching Y Suen. A novel hybrid CNN–SVM classifier for recognizing handwritten digits. *Pattern Recognition*, 45(4):1318–1325, 2012.
- [7] Jayadeva, R. Khemchandani, and S. Chandra. Twin support vector machines for pattern classification. *IEEE Transactions on Pattern Analysis and Machine Intelligence*, 29(5):905–910, 2007.
- [8] MA Ganaie, M. Tanveer, and CT Lin. Large-scale fuzzy least squares twin svms for class imbalance learning. *IEEE Transactions on Fuzzy Systems*, 30(11):4815–4827, 2022. doi: 10.1109/TFUZZ.2022.3161729.
- [9] M. Tanveer, A. Tiwari, R. Choudhary, and MA Ganaie. Large-scale pinball twin support vector machines. *Machine Learning*, pages 1–24, 2022. doi: 10.1007/s10994-021-06061-z.
- [10] M. Tanveer, T. Rajani, R. Rastogi, YH Shao, and MA Ganaie. Comprehensive review on twin support vector machines. *Annals of Operations Research*, pages 1–46, 2022. doi: 10.1007/s10479-022-04575-w.
- [11] Xiaolin Huang, Lei Shi, and Johan AK Suykens. Support vector machine classifier with pinball loss. *IEEE Transactions on Pattern Analysis and Machine Intelligence*, 36(5):984–997, 2013.

[12] J Paul Brooks. Support vector machines with the ramp loss and the hard margin loss. *Operations Research*, 59(2):467–479, 2011.

[13] Guibiao Xu, Zheng Cao, Bao-Gang Hu, and Jose C Principe. Robust support vector machines based on the rescaled hinge loss function. *Pattern Recognition*, 63:139–148, 2017.

[14] Huajun Wang and Yuanhai Shao. Fast generalized ramp loss support vector machine for pattern classification. *Pattern Recognition*, 146:109987, 2024.

[15] A. Kumari, M. Akhtar, M. Tanveer, and Mohd Arshad. Diagnosis of breast cancer using flexible pinball loss support vector machine. *Applied Soft Computing*, page 111454, 2024. doi: 10.1016/j.asoc.2024.111454.

[16] Ming-Zeng Liu, Yuan-Hai Shao, Chun-Na Li, and Wei-Jie Chen. Smooth pinball loss nonparallel support vector machine for robust classification. *Applied Soft Computing*, 98:106840, 2021.

[17] Ahmad Parsian and SNUA Kirmani. Estimation under Linex loss function. In *Handbook of Applied Econometrics and Statistical Inference*, pages 75–98. CRC Press, 2002.

[18] Yue Ma, Qin Zhang, Dewei Li, and Yingjie Tian. LINEX support vector machine for large-scale classification. *IEEE Access*, 7:70319–70331, 2019.

[19] Mushir Akhtar, M. Tanveer, and Mohd. Arshad. RoBoSS: A robust, bounded, sparse, and smooth loss function for supervised learning. *IEEE Transactions on Pattern Analysis and Machine Intelligence*, pages 1–13, 2024. doi: 10.1109/TPAMI.2024.3465535.

[20] Ting Shi and Sugen Chen. Robust twin support vector regression with smooth truncated H ε loss function. *Neural Processing Letters*, 55(7):9179–9223, 2023.

[21] M. Akhtar, M. Tanveer, and Mohd. Arshad. HawkEye: Advancing robust regression with bounded, smooth, and insensitive loss function. *arXiv preprint*, 2024. doi: <https://doi.org/10.48550/arXiv.2401.16785>.

[22] Yunlong Feng, Yuning Yang, Xiaolin Huang, Siamak Mehrkanoon, and Johan AK Suykens. Robust support vector machines for classification with nonconvex and smooth losses. *Neural Computation*, 28(6):1217–1247, 2016.

[23] Peter L Bartlett, Michael I Jordan, and Jon D McAuliffe. Convexity, classification, and risk bounds. *Journal of the American Statistical Association*, 101(473):138–156, 2006.

[24] Tyler Sypherd, Mario Diaz, John Kevin Cava, Gautam Dasarathy, Peter Kairouz, and Lalitha Sankar. A tunable loss function for robust classification: Calibration, landscape, and generalization. *IEEE Transactions on Information Theory*, 68(9):6021–6051, 2022.

[25] Xiaoxi Zhao, Saiji Fu, Yingjie Tian, and Kun Zhao. Asymmetric and robust loss function driven least squares support vector machine. *Knowledge-Based Systems*, 258:109990, 2022.

[26] Léon Bottou, Frank E Curtis, and Jorge Nocedal. Optimization methods for large-scale machine learning. *SIAM Review*, 60(2):223–311, 2018.

[27] Diederik P Kingma and Jimmy Ba. Adam: A method for stochastic optimization. *arXiv preprint arXiv:1412.6980*, 2014.

[28] John Duchi, Elad Hazan, and Yoram Singer. Adaptive subgradient methods for online learning and stochastic optimization. *Journal of Machine Learning Research*, 12(7), 2011.

[29] Tijmen Tieleman and Geoffrey Hinton. Lecture 6.5-RMSprop: Divide the gradient by a running average of its recent magnitude. *COURSERA: Neural Networks for Machine Learning*, 4(2):26–31, 2012.

[30] Francesco Dinuzzo and Bernhard Schölkopf. The representer theorem for Hilbert spaces: a necessary and sufficient condition. *Advances in Neural Information Processing Systems*, 25, 2012.

[31] M Arun Kumar and Madan Gopal. Least squares twin support vector machines for pattern classification. *Expert systems with applications*, 36(4):7535–7543, 2009.

[32] M. Tanveer, A. Sharma, and PN Suganthan. General twin support vector machine with pinball loss function. *Information Sciences*, 494:311–327, 2019.

[33] Qi Si, Zhixia Yang, and Junyou Ye. Symmetric LINEX loss twin support vector machine for robust classification and its fast iterative algorithm. *Neural Networks*, 168:143–160, 2023.

[34] AK Malik, MA Ganaie, M. Tanveer, PN Suganthan, and Alzheimer’s Disease Neuroimaging Initiative. Alzheimer’s disease diagnosis via intuitionistic fuzzy random vector functional link network. *IEEE Transactions on Computational Social Systems*, pages 1–12, 2022. doi: 10.1109/TCSS.2022.3146974.

[35] Dheeru Dua and Casey Graff. UCI machine learning repository. *URL* <http://archive.ics.uci.edu/ml>, 7(1):62, 2017.

- [36] J Derrac, S Garcia, L Sanchez, and F Herrera. KEEL data-mining software tool: Data set repository, integration of algorithms and experimental analysis framework. *J. Mult. Valued Logic Soft Comput.*, 17:255–287, 2015.
- [37] Le Zhang and PN Suganthan. A comprehensive evaluation of random vector functional link networks. *Information Sciences*, 367:1094–1105, 2016.
- [38] Nello Cristianini and John Shawe-Taylor. *An introduction to support vector machines and other kernel-based learning methods*. Cambridge University Press, 2000.
- [39] AP Porsteinsson, RS Isaacson, Sean Knox, MN Sabbagh, and I Rubino. Diagnosis of early alzheimer’s disease: clinical practice in 2021. *The Journal of Prevention of Alzheimer’s Disease*, 8:371–386, 2021.
- [40] B. Richhariya, M. Tanveer, and Alzheimer’s Disease Neuroimaging Initiative. An efficient angle-based universum least squares twin support vector machine for classification. *ACM Transactions on Internet Technology (TOIT)*, 21(3):1–24, 2021.